utilized, as previously reported [13], incubating ASCs in a 15 ml tube for 21 days in DMEM containing 1% FBS supplemented with 6.25 mg/ml insulin, 10 ng/ml TGFβ-1 and 50 nM of ascorbate-2-phosphate. Regular growth medium was used to plate controls. The three lineages were analyzed qualitatively via Nile red (adipogenic), von Kossa (osteogenic) and Alcian blue (chondrogenic) differential staining and gauged quantitatively by AdipoRed assay (Lonza, Basel, Switzerland), Calcium-E test (Wako Pure Chemical Industries Ltd, Osaka, Japan) and micromass diameter.

Healing of diabetic ulcers in mice models

Care of B6-db/db mice (BKS.Cg/Lepr^{db}/m/JCL, 8-week old male) was conducted in accordance with institutional guidelines, using a protocol approved by the Animal Experimental Committee of University of Tokyo. Under general anesthesia (isoflurane inhalation), the B6-db/db mice were depilated and two full-thickness cutaneous wounds (6 mm each) were created on both sides dorsally, using skin punch devices. A donut-shaped silicone splint was then placed to prevent wound contraction and secured by interrupted 6–0 nylon sutures. MCAM prepared from one inguinal fat pad of a wild-type B6 mouse was injected by 29-G needle into four differing points of subcutis at wound peripheries (n = 4). Injection of PBS served as control. Treated wounds and splints were covered by transparent sterile dressings. Wounds were photographed on days 0, 2, 4, 7, 9, 11 and 14, determining their areas by Photoshop CS5 (Adobe Systems, CA, USA).

Statistical analysis

Results were expressed as mean ± standard error of the mean. To compare capacity for multilineage differentiation, Student's *t*-test was applied; and paired *t*-test was invoked for comparing wound sizes. p-values < 0.05 were considered statistically significant.

Results

Microstructure of micronized cellular adipose matrix

After mouse, adipose tissue was morcellated (100–400 μm maximum dimension), suspended in PBS and centrifuged, tissues were separated into yellowish floating adipose tissue (floating fat) and whitish bottom sedimentation (MCAM) (Figure 1A, left). Scanning electron microscopy (SEM) confirmed a scarcity of adipocytes in MCAM, whereas adipocytes were abundant in floating fat (Figure 1A, right). The lobular structure of floating fat was maintained, with MCAM consisting primarily of connective tissue and collagen bundles.

Whole-mount imaging highlighted functional features of MCAM (Figure 1B). As noted by scanning electron microscopy, MCAM was lacking in mature adipocytes (i.e., the large, round WGA$^+$ (wheat germ agglutinin) green cells seen in floating fat). However, Hoechst$^+$ nucleated cells persisted in MCAM at rather high density. In addition, MCAM retained branches and segments of vessels and identifiable capillaries.

Cellular content of SVF isolated from mouse MCAM

Fluorescence-activated cell sorting analyses were performed to delineate cellular composition, once SVFs were individually isolated from floating fat and MCAM through collagenase digestion (Figure 2). SVFs of fat and MCAM were characterized through a combination of surface markers and classified into four subpopulations; hematopoietic cells (mainly white blood cells; CD45$^+$), vascular endothelial cells (CD45$^-$/CD31$^+$/CD34$^+$), ASCs (CD45$^-$/CD31$^-$/CD34$^+$), and other cells (CD45$^-$/CD31$^-$/CD34$^-$). The SVF of floating fat consisted largely of CD45$^-$ nonhematopoietic cells (~75%), with ASCs accounting for half of the nonhematopoietic fraction. The SVF of MCAM contained all four subpopulations (including ASCs) albeit in differing ratios. ASCs accounted for 13% of MCAM-SVF cells, with hematopoietic cells, vascular endothelial cells and other cells constituting 57.9, 0.7 and 28.3%, respectively. The original protocol was designed for optimal adipose digestion, which may explain the less efficient digestion of MCAM connective tissue and its different composition of cells (ASCs and vascular endothelial cells).

Multilineage differentiation capacity of ASCs isolated from human MCAM

MCAM and floating fat were also extracted from the human lipoaspirate. Cultured ASCs derived from human floating fat and MCAM were compared in terms of capacity for differentiating into three mesenchymal lineages: adipogenic, osteogenic and chondrogenic. After 3 weeks of induction, ASCs of both floating fat and MCAM displayed similar degrees of multilineage differentiation. No morphologic differences in Nile red, von Kossa or Alcian blue staining were detected (Figure 3A), nor did quantification of lipid content, calcium deposition and micromass diameter (reflecting adipogenesis, osteogenesis and chondrogenesis, respectively) differ significantly (Figure 3B). Thus, it was indicated that MCAM contained ASCs with similar differentiating capability to those obtained from regular adipose tissue.

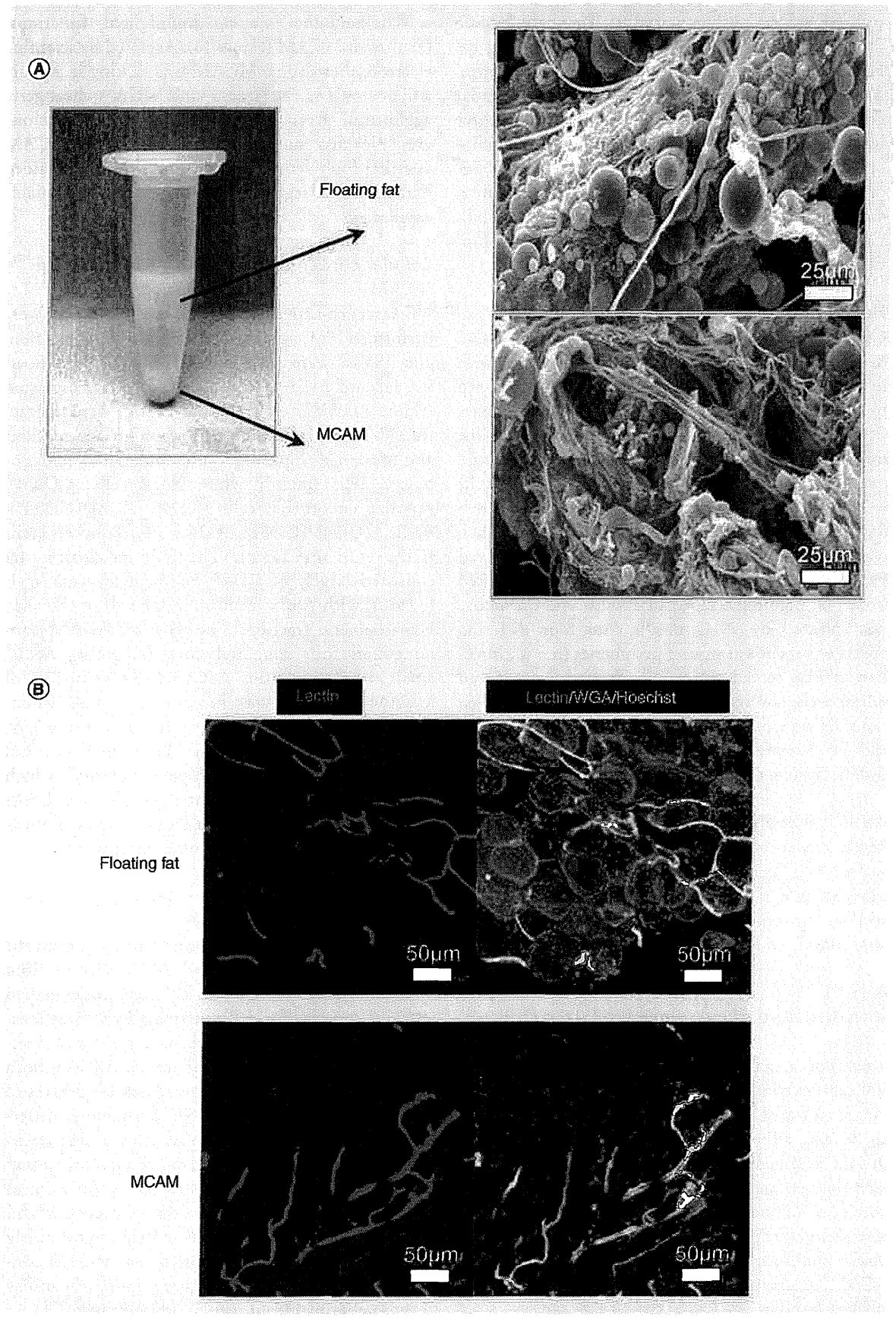
A
Floating fat
MCAM
25μm
25μm
B
Lectin
Lectin/WGA/Hoechst
Floating fat
MCAM
50μm
50μm
50μm
50μm

Figure 1. Microstructure of floating fat and micronized cellular adipose matrix (see facing page). (A) Once minced inguinal fat pad of mouse was centrifuged, micronized cellular adipose matrix (MCAM; whitish sediment) separated from floating fat. Scanning electron microscopy revealed highly fibrous nature of MCAM (vs floating fat), with few mature adipocytes. Bars = 25 μm. **(B)** Whole-mount staining of lectin (vascular endothelial cells: red), wheat germ agglutinin (cell membranes: green) and Hoechst (nuclei: blue); mature adipocytes scarce in MCAM, but microvascular structures in connective tissue remained intact. Bars = 50 μm.
MCAM: Micronized cellular adipose matrix; WGA: Wheat germ agglutinin.
For color images please see online at www.futuremedicine.com/doi/full/10.2217/RME.15.48

Therapeutic effects of mouse MCAM for diabetic ulcers

Subcutis of full-thickness dorsal skin ulcers inflicted in diabetic mice was injected at wound peripheries with MCAM prepared from wild-type mice, using pBS injections as control. Healing of diabetic ulcers was significantly more rapid with MCAM (vs pBS) injection, with 64% smaller wound size on day 4 ($p = 0.0082$) and 65% smaller size on day 7 ($p = 0.0043$; Figure 4). At the close of week 2, closure was essentially completed in MCAM-treated ulcers, whereas wound beds of pBS-treated ulcers remained hyperemic.

Discussion

For this investigation, our injectable MCAM by design was a formulation of bioactive ECM and functional ASCs, prepared by mechanical mincing and elimination of adipocytes from adipose tissue. Sharp-bladed instruments, such as scissors, easily micronized the connective tissue in fat without significantly altering its basic structure, and viability of cells was retained. Approximate specific gravities of human adipocyte and connective tissue obtained from human lipoaspirates were 0.85–0.87 and 1.1–1.2, respectively, underscoring that MCAM regularly sediments upon centrifugation of processed samples.

There is an abundance of evidence affirming the biologic utility of ECM, namely the capacity to regulate proliferation and differentiation of tissue-resident stem cells [14]. Acellular ECM products, whether dermal or fatty by nature, have proven therapeutic in clinical and experimental contexts [9–11,15–16], providing biocompatible substrates or scaffolding and trophic/growth factors needed to accommodate and recruit stem/progenitor cells. In addition to supplying ECM essentials, our MCAM injectable also incorporates an array of viable cells (ASCs, vascular endothelial cells and more) that engage in wound healing.

To date, such scaffolds are designed to mimic native environments, ensuring original cell functions are maintained for optimal cell expansion and tissue regeneration [17–19]. ASCs in MCAM occupy their original ECM niche, ready to assume original roles. As shown by whole-mount staining and flow cytometry, vessels and capillaries of MCAM, as well as ASCs and other stromal cells, retained their natural states and positions. Functional aspects of ASCs in MCAM were also well preserved, as partly indicated by differentiation assays.

ASCs are thought to be potent sources of trophic factors and to have multilineage differentiation capacity. Nonetheless, in transplantation of dissociated (suspended) ASCs, local retention was found to be poor (many disappearing in 1 week), thus nullifying therapeutic intent or resulting in unexpected stem cell behaviors [5,7,20]. As the size of injectable MCAM ranges 100–400 μm, the ECM of MCAM may also provide better mechanical support and anchorage for ASCs to avoid their rapid and seemingly detrimental migration.

Our *in vivo* results suggest that MCAM does impact the healing of diabetic ulcers by accelerating tissue repair. Although similar therapeutic effects have already been reported with use of isolated and cultured ASCs in diabetic or generic refractory ulcers [21–24], substantial procedural manipulations (i.e., enzymatic digestion and isolation or culture of cells) to possibly change biological properties of ASCs are not required for MCAM preparation, eliminating potential regulatory concerns. In skin wound healing models, significant differences are usually observed at a specific and limited time range [25,26], because the skin wound closes eventually in any model (thus no difference at later stages). Our objective was to design a safe and functional injectable, requiring little in the way of preparation. In this study, MCAM obtained from wild-type healthy mice was administered into diabetic mice and it is a limitation of this study that MCAM from diabetic mice was not evaluated. Although ASCs from diabetic patients may not have the same function as those from healthy subjects, ASCs are known to be relatively immunoprivileged and may work as a temporary drug to release trophic factors and help wound healing by allogeneic use.

Fat grafting is claimed to have comparable clinical effects, promoting wound healing of refractory ulcers, such as those seen postirradiation [27–29], and providing a remedy for stem-cell depleted conditions such as chronic ischemia [30,31], systemic sclerosis [32] and scar contracture [33–35]. Improvement of such problematic conditions suggests that the clinical benefits may be partly attributable to functional ASCs. However, if volumetric restoration is not desired, as in transplantations for tissue revitalization/fertilization, the volume occupied by adipocytes within the graft would signifi-

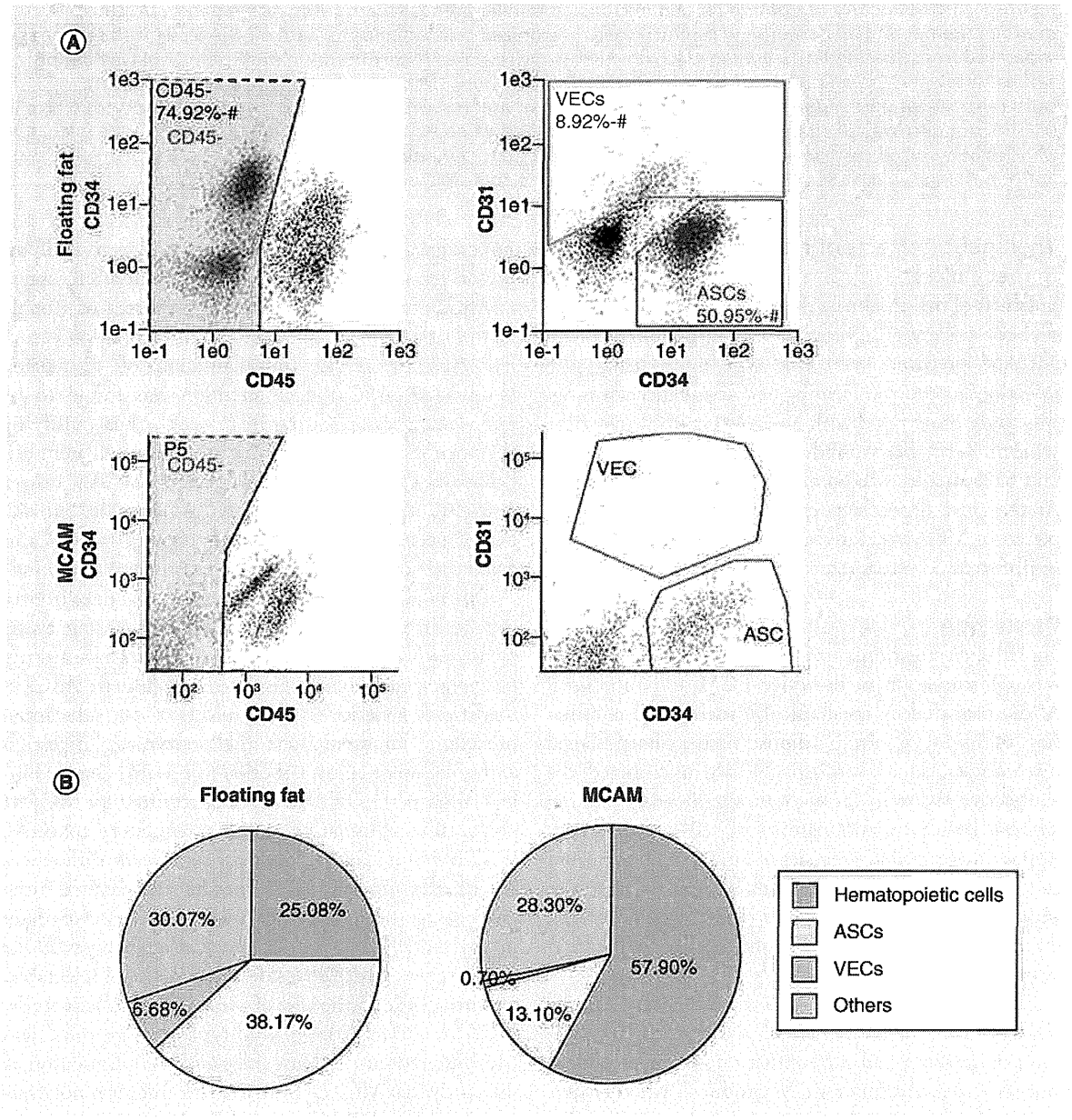

Figure 2. Cellular content of stromal vascular fraction isolated from mouse floating fat and micronized cellular adipose matrix. (A) SVFs from floating fat and that from MCAM were isolated through digestion by collagenase, identifying content as follows: hematopoietic cells (primarily WBCs; $CD45^+$), VECs ($CD45^-/CD31^+/CD34^+$), ASCs ($CD45^-/CD31^-/CD34^+$) and other cells ($CD45^-/CD31^-/CD34^-$). **(B)** ASCs in MCAM account for 13.1% of SVF cells. Hematopoietic cells, VECs and other cells comprise 57.9, 0.7 and 28.3%, respectively. More ASCs (38.2%) and VECs (6.7%) are evident in SVF of floating fat by comparison.
ASC: Adipose-derived stem/stromal cell; MCAM: Micronized cellular adipose matrix; SVF: Stromal vascular fraction; VEC: Vascular endothelial cell.

cantly decrease the density of ASCs and ECM. In these cases, ASCs alone or in conjunction with ECM (as in MCAM) may provide sufficient therapeutic effect, as we have shown.

Conclusion

MCAM is an autologous/allogeneic injectable of bioactive ECM and functional cellular components generated through minimal manipulation of adipose tissue. Smaller-sized and more homogeneous (50–100 μm) particles may be preferable as injectables, but as we already learned, such preparations may jeopardize the viability of cells. Further studies are needed to verify the hypothesized mechanism underlying the efficacy of MCAM and further optimization of preparation methods. Therapeutic effect of MCAM in other stem

cell-depleted states, including irradiation damage and fibrous diseases will also need to be tested. Besides, we still need to elucidate the specific functions of adipocytes in clinical fat grafting and to see what benefits of fat grafting will be lost when we use the product like MCAM, where mature adipocytes are virtually absent. Our efforts here attest to the therapeutic potential of MCAM in ischemic diabetic ulcers, offering a novel mode of tissue repair and revitalization with a minimally invasive approach.

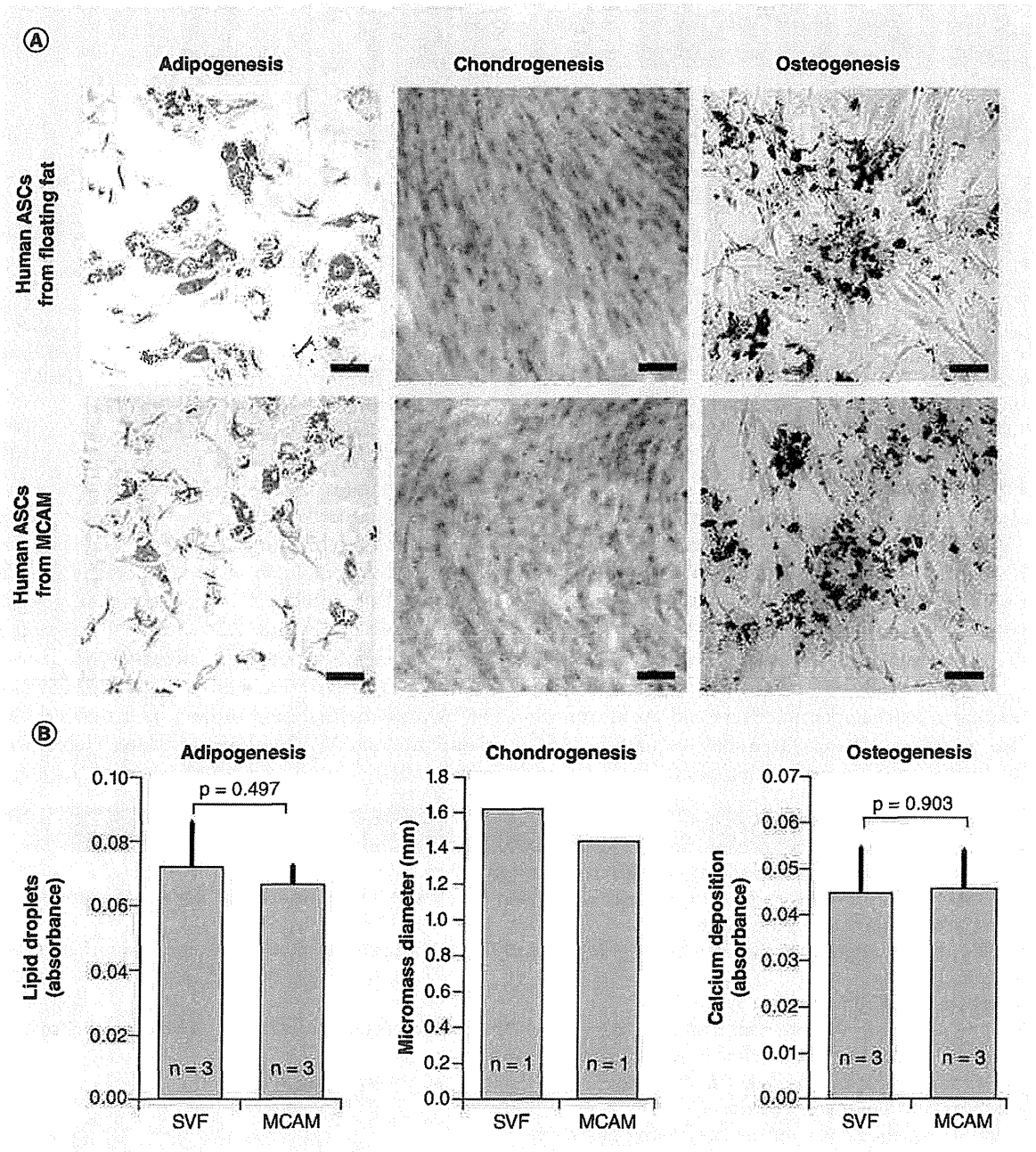

Figure 3. Multilineage differentiation capacity of cultured adipose-derived stem/stromal cells isolated from human floating fat and micronized cellular adipose matrix. (A) Microscopic images of differential induction: cultured human ASCs of floating fat and MCAM yielded similar adipogenic, chondrogenic and osteogenic differentiation; lineage-specific differentiation delineated by Nile red, Alcian blue and von Kossa stains, respectively. Scale bar = 100 μm. **(B)** Quantitative analysis of cellular differentiation: capacity for multilineage differentiation, as indicated by accumulated lipid (adipogenesis), micromass diameter (chondrogenesis) and calcium deposition (osteogenesis), showing no significant differences between fractions. ASC: Adipose-derived stem/stromal cell; MCAM: Micronized cellular adipose matrix; SVF: Stromal vascular fraction.

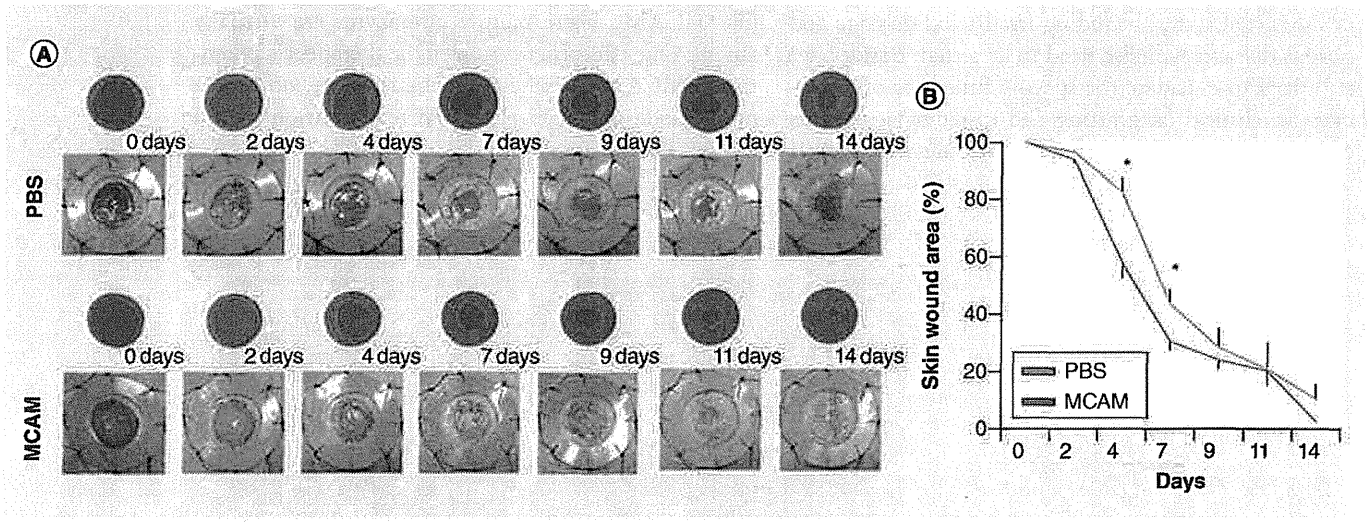

Figure 4. Therapeutic mouse micronized cellular adipose matrix injection of diabetic ulcers. **(A)** Representative photos of cutaneous wounds (6 mm) created on dorsal areas of diabetic (db/db) mice (n = 4) and treated by local injection of PBS or MCAM on day 0, with 2-week follow-up; ulcerated surface areas determined via software. **(B)** Comparison of wound surface areas (determined digitally): significantly reduced ulcer size in MCAM-injected mice (vs PBS-injected controls), day 4 ($p = 0.0082$) and day 7 ($p = 0.0432$).
MCAM: Micronized cellular adipose matrix; PBS: Phosphate-buffered saline.

Future perspective

Regulatory organizations in many countries regard SVF isolated from adipose tissue as a 'more than minimal manipulated' biological drug, of which uses are strictly regulated due to its associated safety issues. Although therapeutic potential of ASCs in the SVF was extensively studied, cell suspension of ASCs may not be the optimal means in order to maximize its therapeutic effects and avoid unfavorable migration. If injectable tools containing ASCs can be prepared through minimal manipulation and show comparable therapeutic effects, it would be a potential alternative. Also, as ASCs are relatively immunoprivileged, allogeneic ASCs may be clinically used, for example, as a temporarily-working drug to release cytokines. It may be a good news for diseased patients whose ASCs cannot function as those of healthy patients. In this study, we focused on the characterization and therapeutic effects of MCAM as the first step to develop a new cellular/tissue product. MCAM accommodates viable ASCs within their natural niche and may be valuable in

Executive summary

Micronized cellular adipose matrix definition and preparation

- MCAM is the abbreviation for micronized cellular adipose matrix. It is an injectable cellular matrice product extracted from the adipose tissue.
- MCAM is obtained as the pelleted material from centrifugation after finely mincing and fragmentation of fat tissue.

Microstructure of MCAM

- Comparing with the intact fat tissue, MCAM includes few adipocytes but a substantial number of adipose derived stem cells (ASCs) within its abundant connective tissue.
- *Microvascular structures in extracellular connective tissue of MCAM remained intact.*

Analysis of cellular composition

- MCAM retained ASCs and vascular endothelial cells.
- ASCs within MCAM were viable and maintained similar mesenchymal differentiation capacity compared to those ASCs obtained through the standard collagenase digestion method.

Regenerative potential

- In diabetic mice model, excisional skin wounds treated with MCAM showed accelerated healing compared to phosphate-buffered saline-treated wounds.

Conclusion

- MCAM is an injectable tissue product contains both functional stem cells and extracellular matrix. MCAM is prepared through minimal manipulation and thus can be readily used without regulatory issues. MCAM may offer a safe and effective option in chronic wound repair and tissue revitalization.

treating stem cell-depleted conditions such as chronically inflammated tissues/ulcers and radiated tissue damage. Another future study is needed to explore the effectiveness of MCAM compared with other cellular formulations such as freshly isolated SVF and cultured ASCs.

Financial & competing interests disclosure

This study was supported by the Japanese Ministry of Education, Culture, Sports, Science and Technology (MEXT); contract grant number: Grant-in-Aid for Scientific Research B3-24390398. The authors have no other relevant affiliations or financial involvement with any organization or entity with a financial interest in or financial conflict with the subject matter or materials discussed in the manuscript apart from those disclosed.

No writing assistance was utilized in the production of this manuscript.

Ethical conduct of research

The authors state that they have obtained appropriate institutional review board approval or have followed the principles outlined in the Declaration of Helsinki for all human or animal experimental investigations. In addition, for investigations involving human subjects, informed consent has been obtained from the participants involved.

References

Papers of special note have been highlighted as:
• of interest

1 Yoshimura K, Suga H, Eto H. Adipose-derived stem/progenitor cells: roles in adipose tissue remodeling and potential use for soft tissue augmentation. *Regen. Med.* 4(2), 265–273 (2009).

2 Yoshimura K, Eto H, Kato H *et al. In vivo* manipulation of stem cells for adipose tissue repair/reconstruction. *Regen. Med.* 6(6 Suppl.), 33–41 (2011).

3 Gentile P, Orlandi A, Scioli MG *et al.* A comparative translational study: the combined use of enhanced stromal vascular fraction and platelet-rich plasma improves fat grafting maintenance in breast reconstruction. *Stem Cells Transl. Med.* 1(4), 341–351 (2012).

4 Kølle SF, Fischer-Nielsen A, Mathiasen AB *et al.* Enrichment of autologous fat grafts with *ex-vivo* expanded adipose tissue-derived stem cells for graftsurvival: a randomised placebo-controlled trial. *Lancet* 382(9898), 1113–1120 (2013).

5 Yoshimura K, Aoi N, Suga H *et al.* Ectopic fibrogenesis induced by transplantation of adipose-derived progenitor cell suspension immediately after lipoinjection. *Transplantation* 85(12), 1868–1869 (2008).

• **A clinical report of unfavorable stem cell migration and differentiation called for attention to the possible risk of local injection of stromal vascular fraction cell suspension.**

6 Yamada Y, Nakamura S, Ito K *et al.* Injectable tissue-engineered bone using autogenous bone marrow-derived stromal cells for maxillary sinus augmentation: clinical application report from a 2–6-year follow-up. *Tissue Eng. Part A* 14(10), 1699–1707 (2008).

7 Cheng NC, Wang S, Young TH. The influence of spheroid formation of human adipose-derived stem cells on chitosan films on stemness and differentiation capabilities. *Biomaterials* 33(6), 1748–1758 (2012).

8 Matsuura K, Utoh R, Nagase K *et al.* Cell sheet approach for tissue engineering and regenerative medicine. *J. Control. Release* 190, 228–239 (2014).

9 Vorotnikova E, McIntosh D, Dewilde A *et al.* Extracellular matrix-derived products modulate endothelial and progenitor cell migration and proliferation *in vitro* and stimulate regenerative healing *in vivo*. *Matrix Biol.* 29(8), 690–700 (2010).

10 Novitsky YW, Rosen MJ. The biology of biologics: basic science and clinical concepts. *Plast. Reconstr. Surg.* 130(5 Suppl. 2), S9–S17 (2012).

11 Iorio ML, Shuck J, Attinger CE. Wound healing in the upper and lower extremities: a systematic review on the use of acellular dermal matrices. *Plast. Reconstr. Surg.* 130(5 Suppl. 2), S232–S241 (2012).

12 Halme DG, Kessler DA. FDA regulation of stem-cell-based therapies. *N. Engl. J. Med.* 355(16), 1730–1735 (2006).

13 Umeda K, Zhao J, Simmons P *et al.* Human chondrogenic paraxial mesoderm, directed specification and prospective isolation from pluripotent stemcells. *Sci. Rep.* 2, 455 (2012).

14 Discher DE, Mooney DJ, Zandstra PW. Growth factors, matrices, and forces combine and control stem cells. *Science* 324(5935), 1673–1677 (2009).

15 Choi JS, Yang HJ, Kim BS *et al.* Fabrication of porous extracellular matrix scaffolds from human adipose tissue. *Tissue Eng. Part C Methods* 16(3), 387–396 (2010).

• **The study first showed the function and potential use of decellularized extracellular matrix from adipose tissue for regenerative medicine.**

16 Sano H, Orbay H, Terashi H *et al.* Acellular adipose matrix as a natural scaffold for tissue engineering. *J. Plast. Reconstr. Aesthet. Surg.* 67(1), 99–106 (2014).

17 Li Y, Liu W, Liu F *et al.* Primed 3D injectable microniches enabling low-dosage cell therapy for critical limb ischemia. *Proc. Natl Acad. Sci. USA* 111(37), 13511–13516 (2014).

18 Lin CS, Xin ZC, Deng CH *et al.* Defining adipose tissue-derived stem cells in tissue and in culture. *Histol. Histopathol.* 25(6), 807–815 (2010).

19 Yang G, Rothrauff BB, Lin H *et al.* Enhancement of tenogenic differentiation of human adipose stem cells by tendon-derived extracellular matrix. *Biomaterials* 34(37), 9295–9306 (2013).

20 Park IS, Chung PS, Ahn JC. Enhanced angiogenic effect of adipose-derived stromal cell spheroid with low-level light therapy in hind limb ischemia mice. *Biomaterials* 35(34), 9280–9289 (2014).

21 Amos PJ, Kapur SK, Stapor PC *et al.* Human adipose-derived stromal cells accelerate diabetic wound healing: impact of cell formulation and delivery. *Tissue Eng. Part A* 16(5), 1595–1606 (2010).

22 Tanaka R, Vaynrub M, Masuda H *et al.* Quality-control culture system restores diabetic endothelial progenitor cell vasculogenesis and accelerates wound closure. *Diabetes* 62(9), 3207–3217 (2013).

23 Ebrahimian TG, Pouzoulet F, Squiban C *et al.* Cell therapy based on adipose tissue-derived stromal cells promotes physiological and pathological wound healing. *Arterioscler. Thromb. Vasc. Biol.* 29(4), 503–510 (2009).

24 Han SK, Kim HR, Kim WK. The treatment of diabetic foot ulcers with uncultured, processed lipoaspirate cells: a pilot study. *Wound Repair Regen.* 18(4), 342–348 (2014).

25 Kim EK, Li G, Lee TJ *et al.* The effect of human adipose-derived stem cells on healing of ischemic wounds in a diabetic nude mouse model. *Plast. Reconstr. Surg.* 128(2), 387–394 (2011).

26 Zografou A, Papadopoulos O, Tsigris C *et al.* Autologous transplantation of adipose-derived stem cells enhances skin graft survival and wound healing in diabetic rats. *Ann. Plast. Surg.* 71(2), 225–232 (2013).

27 Rigotti G, Marchi A, Galiè M *et al.* Clinical treatment of radiotherapy tissue damage by lipoaspirate transplant: a healing process mediated by adipose-derived adult stem cells. *Plast. Reconstr. Surg.* 119(5), 1409–1422 (2007).

28 Phulpin B, Gangloff P, Tran N *et al.* Rehabilitation of irradiated head and neck tissues by autologous fat transplantation. *Plast. Reconstr. Surg.* 123(4), 1187–1197 (2009).

29 Salgarello M, Visconti G, Barone-Adesi L. Fat grafting and breast reconstruction with implant: another option for irradiated breast cancer patients. *Plast. Reconstr. Surg.* 129(2), 317–329 (2012).

30 Klinger M, Caviggioli F, Vinci V *et al.* Treatment of chronic posttraumatic ulcers using autologous fat graft. *Plast. Reconstr. Surg.* 126(3), e154–e155 (2010).

31 Marangi GF, Pallara T, Cagli B *et al.* Treatment of early-stage pressure ulcers by using autologous adipose tissue grafts. *Plast. Surg. Int.* 2014, 817283 (2014).

32 Del Papa N, Caviggioli F, Sambataro D *et al.* Autologous fat grafting in the treatment of fibrotic perioral changes in patients with systemic sclerosis. *Cell Transplant.* 24(1), 63–72 (2015).

33 Caviggioli F, Maione L, Forcellini D *et al.* Autologous fat graft in postmastectomy pain syndrome. *Plast. Reconstr. Surg.* 128(3), 349–352 (2011).

34 Mazzola IC, Cantarella G, Mazzola RF. Management of tracheostomy scar by autologous fat transplantation: a minimally invasive new approach. *J. Craniofac. Surg.* 24(4), 1361–1364 (2013).

35 Pallua N, Baroncini A, Alharbi Z *et al.* Improvement of facial scar appearance and microcirculation by autologous lipofilling. *J. Plast. Reconstr. Aesthet. Surg.* 67(8), 1033–1037 (2014).

Clinicopathologic Assessment of Myositis Ossificans Circumscripta of the Masseter Muscles

To the Editor: Myositis ossificans (MO) is a heterotopic bone formation within the muscle, and can be classified into 3 subtypes: fibrodysplasia ossificans progressiva, neurogenic MO, and traumatic MO circumscripta, which is a benign and reactive bone formation within the muscle after trauma. Traumatic MO circumscripta mostly occurs in the thigh and brachium,[1] and the occurrence in the masticatory muscles, though rare, usually results in temporomandibular joint dysfunction. Although the exact cause of MO circumscripta remains unknown, it has been presumed that infection, hematoma, tearing of the periosteum and bony metaplasia of the muscle and fibrous connective tissues cause heterotopic ossification.[2]

A 36-year-old man experiencing severe trismus was referred to our hospital. He was, at the age of 21, under confinement for 1 year and frequently abused about the face. On physical examination, maximal interincisal distance (MID) was 10 mm and hard masses were palpated in the bilateral cheeks (Fig. 1). Computed tomography scan showed calcified masses in the bilateral masseter muscles extending from the zygomatic arch to the ascending ramus of the mandible (Fig. 1). He was diagnosed as MO circumscripta, and as the disease state had not been progressive for the past several years, surgical intervention was selected to alleviate the trismus.

We performed bilateral osteotomies of the bony fragments, and bilateral coronoidectomies to eliminate any possibility of further restriction of the jaw function. Following this, gentle manipulation of the jaw resulted in a full range of motion, achieving an MID of 40 mm, and the wound was closed in layers. The day after the operation, the patient's trismus was temporarily aggravated probably because of postoperative edema and pain in the masseter region. After 2 months of physical therapy, the patient, however, presented an MID of 36 mm (Fig. 1). And, as of 1 year after the operation, there was no recurrence of trismus or heterotopic ossification, providing a high level of patient satisfaction and a good functionality.

The most common treatment of MO circumscripta is excision of the lesion or osteotomy, though exacerbation or repeated relapses may occur in some patients.[3] Two successive phases of the disease are known: an early phase with abundant primary vascular cells and angiogenesis, and an ossification phase with premature ectopic bone formation.[1] To prevent recurrence, surgical intervention is recommended after the end of ossification phase. In addition to the removal of a mass, coronoidectomy, or at least coronoidotomy, can be the choice of treatment to eliminate possibility of disturbances in jaw movements.

PATHOLOGIC ASSESSMENT

The pathologic examination of the decalcified, hematoxylin–eosin stained specimens revealed that the ossified mass had a dense and rigid bony structure of mature lamellar bone, including Haversian systems and bone trabeculae (Fig. 1). This indicates osteogenesis was once dynamic though later subsided. Moreover, most interestingly, there were striate muscles between the trabeculae, where bone marrow is normally present. This suggests that osteogenesis was induced along existing masseter muscles, presumably by muscle-derived stem cells differentiating into osteoblasts.[4] There, however, remains a slight possibility of migration of marrow-derived stem cells into the muscle region.

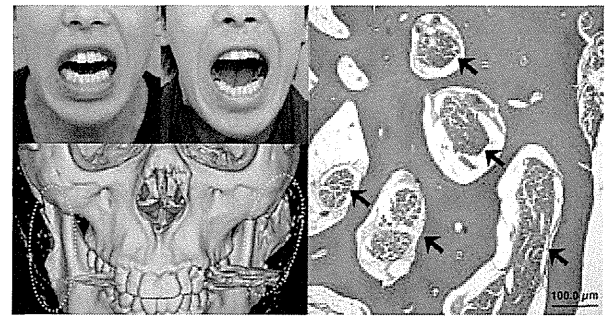

FIGURE 1. The maximal interincisal distance improved from 10 mm (before treatment) to 36 mm (2 months postoperatively). Preoperative 3D-CT images revealed large ossified masses in the masseter region of the left and right sides (50 and 21 mm in maximum diameter, respectively). Pathologic findings of the left ossified mass (hematoxylin and eosin stain) showed that rigid bony structure constituted a large portion of the specimen, and striate muscles (black arrow) existed between bone trabeculae where bone marrow is normally present. 3D-CT, three-dimensional computed tomography.

Takanobu Mashiko, MD
Department of Plastic Surgery
Tokyo Metropolitan Police Hospital
Nakano, Nakano-Ku
Tokyo, Japan
takanobu-mashiko@umin.ac.jp

Tanetaka Akizuki, MD
Yorikatsu Watanabe, MD
Department of Plastic Surgery
Tokyo Metropolitan Police Hospital
Nakano-ku, Tokyo, Japan

Ryo Sasaki, DDS
Department of Plastic Surgery
Tokyo Women's Medical University
School of Medicine
Shinjuku-ku, Tokyo, Japan

Munehiro Yokoyama, MD
Department of Pathology
Tokyo Metropolitan Police Hospital
Nakano, Nakano-Ku, Tokyo, Japan

Kotaro Yoshimura, MD
Kazuhide Mineda, MD
Department of Plastic Surgery
University of Tokyo
School of Medicine
Hongo, Bunkyo-Ku, Tokyo, Japan

REFERENCES

1. Godhi SS, Singh A, Kukreja P, et al. Myositis ossificans circumscripta involving bilateral masticatory muscles. *J Craniofac Surg* 2011;22:e11–e13
2. Molloy JC, McGuirk RA. Treatment of traumatic myositis ossificans circumscripta: use of aspiration and steroids. *J Trauma* 1976;16:851–857
3. Aoki T, Naito H, Ota Y, et al. Myositis ossificans traumatica of the masticatory muscles: review of the literature and report of a case. *J Oral Maxillofac Surg* 2002;60:1083–1088
4. Shi X, Garry DJ. Muscle stem cells in development, regeneration, and disease. *Genes Dev* 2006;20:1692–1708

Perpendicular Strut Injection of Hyaluronic Acid Filler for Deep Wrinkles

Takanobu Mashiko, MD*
Kahori Kinoshita, MD*
Koji Kanayama, MD*
Jingwei Feng, MD*
Kotaro Yoshimura, MD*†

Summary: Although various injection techniques of hyaluronic acid (HA) filler for facial rejuvenation have been developed, correction of deep wrinkles/grooves, such as the nasolabial fold (NLF), with intradermal or subdermal injections remains difficult. We tested the intradermal HA injection method to place multiple HA struts by (1) inserting a small needle perpendicularly to the wrinkle and (2) injecting HA as intradermal struts with the skin fully stretched by the practitioner's fingers. The results of both NLFs in 10 patients suggest that this technique improves NLFs and maintain the effects more consistently than conventional techniques, although the effects of both methods were almost lost after 6 months. Selective and/or combined application of this technique may enhance the current approach to facial rejuvenation with dermal fillers. *(Plast Reconstr Surg Glob Open 2015;3:e567; doi: 10.1097/GOX.0000000000000552; Published online 20 November 2015.)*

Various techniques of hyaluronic acid (HA) filler injection have been developed, such as the serial puncture, linear threading, fanning, cross-hatching, and tower technique.[1,2] An optimal injection technique depends on the filling agent, the area and target to be corrected, and preference of the surgeon. The differential use of these techniques is a key to maximizing aesthetic results. Intradermal injection is a basic approach to treat deep wrinkles; however, occasionally, unfavorable results are encountered, such as conspicuous ridging or beading on or adjacent to the target wrinkle[3] and negligible effects on wrinkles. Deep wrinkles/grooves accompanied with ptosis of the soft tissue are often not fully corrected by a single procedure and may need to be treated by a combination of intradermal and subdermal injections. To provide more consistent intradermal structural support, we tested an intradermal injection technique to place "multiple perpendicular struts" of HA. Herein, we report the clinical benefit suggested by this study.

*From the *Department of Plastic Surgery, University of Tokyo, School of Medicine, Tokyo Japan; and †Department of Plastic Surgery, Jichi Medical University, Shimotsuke, Japan.*
Received for publication March 31, 2015; accepted October 6, 2015.

DOI: 10.1097/GOX.0000000000000552

PATIENTS AND METHODS

Study Patients

Ten consecutive patients (9 women and 1 man), between the age of 39 and 67 years (mean, 50.2 years), were enrolled in this study with an informed consent approval by the institutional review board. In terms of inclusion criteria, healthy adult patients were required to have bilateral nasolabial fold (NLF) ratings of 2 (mild) to 4 (severe) on the 5-grade Wrinkle Severity Rating Scale (WSRS) (Table 1) and be willing to abstain from other cosmetic procedures

Disclosure: *The authors have no financial interest to declare in relation to the content of this article. The Article Processing Charge was paid for by the authors.*

Supplemental digital content is available for this article. Clickable URL citations appear in the text.

for the duration of the study. The exclusion criteria included a history of facial rejuvenation treatments in the previous 6 months.

Injection Materials and Procedure

A cross-linked HA (Restylane, Q-MED AB, Uppsala, Sweden) was injected through a sharp 30-gauge needle. Each patient received HA injections to the bilateral NLFs using either the "perpendicular strut technique" or the linear threading and fanning techniques (which are traditionally used for NFL treatment[1]). The same amount of HA was used for both sides (between 0.3 and 0.5 mL for each side, depending on the severity of the NLF rating); overcorrection was not allowed.

For the "perpendicular strut" technique, HA struts (10–12 mm long) were intradermally delivered in a direction perpendicular to NLF (Fig. 1). The needle was placed almost horizontally to the skin surface and perpendicular to the nasolabial fold and then inserted (its entire length of 0.5 in.) into the mid to deep dermis (with the skin fully stretched by the practitioner's fingers) in a direction perpendicular to the NLF. HA was introduced into the dermis during withdrawal of the needle, creating "struts" consisting of 0.01–0.03 mL HA. (See video, Supplemental Digital Content 1, which displays the injection technique. http://links.lww.com/PRSGO/A150.) Fifteen to 30 struts of HA were spread over the NLF area, and the spacing between each strut was approximately 1 mm. After releasing the fingers from the skin, multiple HA struts gave structural support to maintain the skin partly stretched. The same amount of HA was also injected into the other side, using conventional linear threading and fanning techniques. Patients were randomized regarding which side of the NLF would be injected using the strutting or conventional technique. No compensation was conducted even when 1 side had worse NFL and the same amount of HA gel was used on each side. Although the injector was not blinded to the injection method, the patient and the evaluators were blinded. Gentle massage of the treated area after injection was recommended on both sides. The initial treatment was followed without any touch-up treatment.

Evaluation of Results

WSRS scoring was performed to measure effectiveness by 3 blinded, certified plastic surgeons. The NLF was graded before, 4, and 24 weeks after treatment through the comparison of photographs. The paired t test was used to compare improvements in WSRS score on each side. The blinded evaluators also answered the query, "which side had better improvement, judging from comparison of before and after photographs." The query results were analyzed with χ^2 test. Safety and efficacy were measured by physician assessment and use of

Table 1. Wrinkle Severity Rating Scale

Score	Description
5	Extreme: extremely deep and long folds, detrimental to facial appearance; 2- to 4-mm visible V-shaped folds when stretched
4	Severe: very long and deep folds; prominent facial features; less than 2 mm visible when stretched
3	Moderate: moderately deep folds; clear facial features visible at normal appearance but not when stretched
2	Mild: shallow but visible folds with a slight indentation; minor facial features
1	Absent: no visible folds; continuous skin line

Cited from the work of Narins et al.[4]

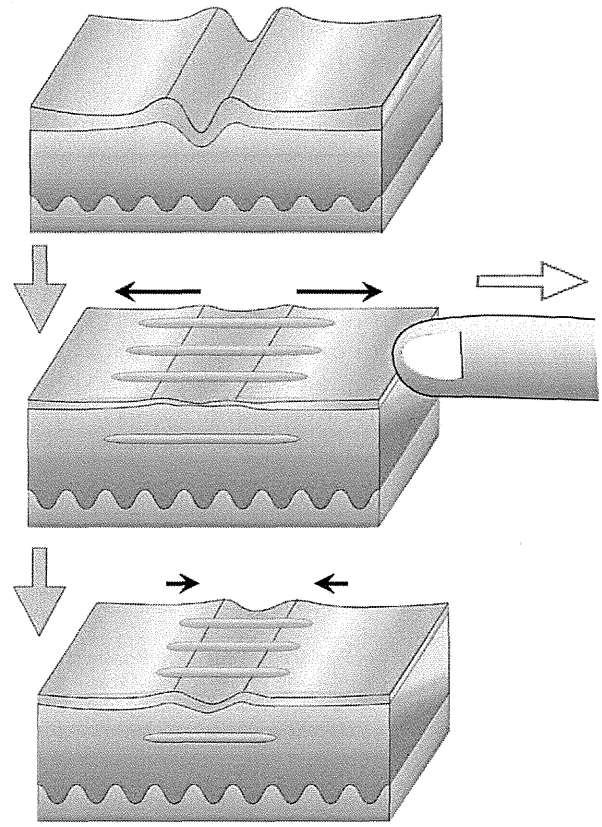

Fig. 1. Scheme of "perpendicular strut injection." The needle is placed almost horizontally to the skin surface and perpendicularly to the nasolabial fold. It is inserted into the dermis for the entire needle length (0.5 in.) with the skin fully stretched using fingers. Hyaluronic acid (HA) is introduced into the dermis while withdrawing the needle, creating a "strut" of 0.03–0.05 mL HA. After the release of the fingers, HA struts give supportive forces to the skin to allow it to be stretched to some extent.

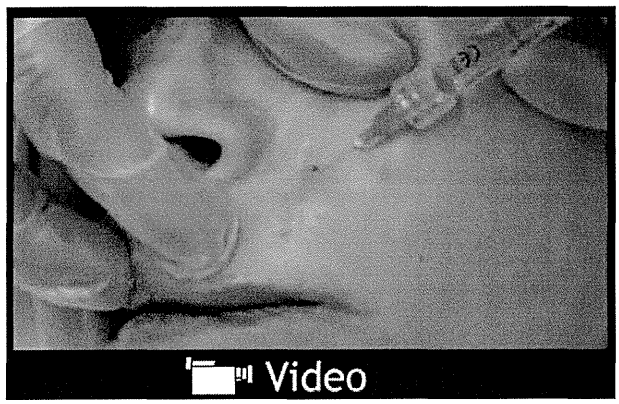

Video Graphic 1. See video, Supplemental Digital Content 1, which displays the injection technique. http://links.lww.com/PRSGO/A150.

patient diaries recording adverse events for 2 weeks after treatment.

RESULTS

All 10 patients completed the study. Mean and individual scores using the WSRS system are shown in Table 2. Four weeks after treatment, grade improvement was significantly greater in the strut method (1.7) than in the conventional side method (1.3; $P = 0.036$). Twenty-four weeks after treatment, improvement from baseline almost disappeared on the both sides. In addition, the query results answered by the 3 blinded evaluators are shown in Table 3. Significant difference was observed at 4 weeks after treatment ($P < 0.01$) but not at 24 weeks after treatment ($P > 0.05$). Temporary adverse events are shown in Table 4 and all disappeared within 2 weeks. No other serious complications occurred. Photographs of a representative patient are shown in Figures 2, 3.

Table 2. Wrinkle Severity Rating Scale Data from 10 Patients

	Pre-treatment Grade		Posttreatment Grade after 4 Wk (Grade Improvement)		Posttreatment Grade after 24 Wk (Grade Improvement)	
Patient	Strut	Control	Strut	Control	Strut	Control
1	3	3	2 (1)	2 (1)	3 (0)	3 (0)
2	2	2	1 (1)	1 (1)	2 (0)	2 (0)
3	3	3	1 (2)	1 (2)	2 (1)	3 (0)
4	3	3	1 (2)	2 (1)	3 (0)	3 (0)
5	4	3	2 (2)	2 (1)	3 (1)	3 (0)
6	4	4	2 (2)	2 (2)	4 (0)	3 (1)
7	3	3	1 (2)	2 (1)	3 (0)	3 (0)
8	2	3	1 (1)	2 (1)	2 (0)	2 (1)
9	4	4	2 (2)	2 (2)	4 (0)	4 (0)
10	3	3	1 (2)	2 (1)	3 (0)	3 (0)
Mean	3.1	3.1	1.4 (1.7)	1.8 (1.3)	2.9 (0.2)	2.9 (0.2)

Strut: perpendicular strut technique.
Control: linear threading and fanning technique.

Table 3. Evaluation of Improvement

	4 Wk	24 Wk
Strut	15	7
Control	3	1
Neither	12	22
Total	30	30

Three blinded investigators evaluated 10 patients and answered the query; which side showed better improvement by comparison of before and after photographs.
Strut: perpendicular strut technique.
Control: linear threading and fanning technique.

Table 4. Adverse Events

Adverse Event	Strut (n = 10)	Control (n = 10)
Erythema	2	1
Bruising	1	3
Swelling	2	1
Pain	0	1
Numbness	1	1
Induration	4	1

Strut: perpendicular strut technique.
Control: linear threading and fanning technique.

DISCUSSION

The NLF is composed of deep, firm fibrous tissue that receives terminal muscle fibers from the levators of the upper lip and is deepened by downward displacement of the cheek tissues.[5] HA fillers are now the gold standard in dermal wrinkle repair; however, the result of dermal fillers for NLF remains far from perfect. HA struts placed perpendicularly to the NLFs can give a supporting and sustaining force and stretch the skin against the original wrin-

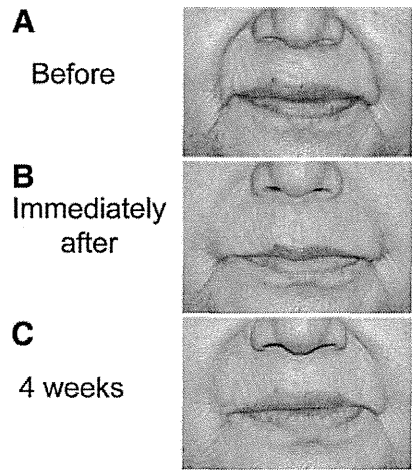

Fig. 2. A 67-year-old woman (patient 10) who underwent intradermal perpendicular strut injection to the right nasolabial fold and the conventional linear threading and fanning injection to the left nasolabial fold, using a total of 0.5 mL HA on each side: (A) before, (B) immediately after treatment, and (C) after 4 weeks; the right side showed better improvement than the left side.

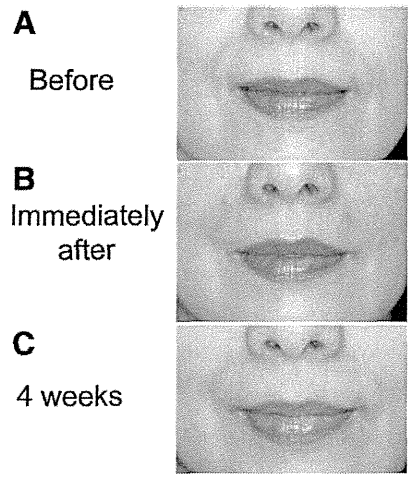

Fig. 3. A 58-year-old woman (patient 2) who underwent intradermal perpendicular strut injection to the left nasolabial fold and the conventional linear threading and fanning injection to the right nasolabial fold, using a total of 0.5 mL HA on each side: (A) before, (B) immediately after treatment and (C) after 4 weeks; the originally more severe left side maintained better improvement than the right side.

kle structure and gravitational descent, although the effect is not permanent. We need to place multiple long struts in the dermis using a hard-type cross-linked HA substance to consistently maximize its effect and stability.

The difference in the results derived from the conventional technique was generally subtle; however, the results suggested that the strut injection technique more consistently achieved sufficient improvement. Because of the degradable property of HA products, aesthetic improvement cannot be sustained for 6 months on either side, and repeated injections are required to maintain the condition. The complication rate is not very different between the 2 sides, except for temporary induration, which more frequently accompanies strut injection (which all diminished within 2 weeks and thus did not affect the outcome at 4-week follow-up). Skin necrosis, because of arterial embolization of the angular branch of the facial artery,[6] never occurs by intradermal injection. Although the small number of patients is a limitation of this study, this is a split-face comparative study, and the obtained findings are well supported by our preliminary experience on this technique in hundreds of patients. Further studies are required to confirm in a large number of patients and determine a good indication of this technique.

Although we treated only NLF in this study, intradermal perpendicular strut injection can be applied to other major facial lines, particularly when conventional injections only work minimally. The strut technique can complement other techniques; for example, an additional volumizing HA injection onlay to the maxillary bone can give sustainable structural support to elevate the entire tissue (skin and subcutaneous tissue),[7] whereas intradermal HA struts can maintain the stretched status of the wrinkled skin.

CONCLUSIONS

Intradermal perpendicular strut injection for the treatment of NLF has proven to be a useful alternative that can give better intradermal structural support for the stretched state of wrinkles. The selective and/or combined application of this technique may enhance the current approach to facial rejuvenation with dermal fillers.

Kotaro Yoshimura, MD
Department of Plastic Surgery
Jichi Medical University
3311-1, Yakushiji, Shimotsuke, 329-0498
Tochigi, Japan
E-mail: kotaro-yoshimura@umin.ac.jp

REFERENCES

1. Rohrich RJ, Ghavami A, Crosby MA. The role of hyaluronic acid fillers (Restylane) in facial cosmetic surgery: review and technical considerations. *Plast Reconstr Surg.* 2007;120(6 Suppl):41S–54S.
2. Carruthers J, Rzany B, Sattler G, et al. Anatomic guidelines for augmentation of the cheek and infraorbital hollow. *Dermatol Surg.* 2012;38(7 Pt 2):1223–1233.
3. Duffy DM. Complications of fillers: overview. *Dermatol Surg.* 2005;31(11 Pt 2):1626–1633.
4. Narins RS, Brandt F, Leyden J, et al. A randomized, double-blind, multicenter comparison of the efficacy and tolerability of Restylane versus Zyplast for the correction of nasolabial folds. *Dermatol Surg.* 2003;29:588–595.
5. Rubin LR, Mishriki Y, Lee G. Anatomy of the nasolabial fold: the keystone of the smiling mechanism. *Plast Reconstr Surg.* 1989;83:1–10.
6. Inoue K, Sato K, Matsumoto D, et al. Arterial embolization and skin necrosis of the nasal ala following injection of dermal fillers. *Plast Reconstr Surg.* 2008;121:127e–128e.
7. Mashiko T, Mori H, Kato H, et al. Semipermanent volumization by an absorbable filler: onlay injection technique to the bone. *Plast Reconstr Surg Glob Open.* 2013;1:e4–e14.

Published Ahead of Print on October 22, 2015 as 10.5966/sctm.2015-0037.

STEM CELLS TRANSLATIONAL MEDICINE®

TISSUE ENGINEERING AND REGENERATIVE MEDICINE

Therapeutic Potential of Human Adipose-Derived Stem/Stromal Cell Microspheroids Prepared by Three-Dimensional Culture in Non-Cross-Linked Hyaluronic Acid Gel

KAZUHIDE MINEDA,[a,b] JINGWEI FENG,[a] HISAKO ISHIMINE,[c,d] HITOMI TAKADA,[d] KENTARO DOI,[a] SHINICHIRO KUNO,[a] KAHORI KINOSHITA,[a] KOJI KANAYAMA,[a] HARUNOSUKE KATO,[a] TAKANOBU MASHIKO,[a] ICHIRO HASHIMOTO,[b] HIDEKI NAKANISHI,[b] AKIRA KURISAKI,[d] KOTARO YOSHIMURA[a,e]

Key Words. Three-dimensional culture • Non-cross-linked hyaluronic acid • Adipose-derived stem/stromal cells • Spheroids • Ischemia-reperfusion injury • Muse cells • Floating culture • Wound healing • Angiogenesis • Vascular endothelial cells

[a]Department of Plastic Surgery, School of Medicine, University of Tokyo, Tokyo, Japan; [b]Department of Plastic Surgery, School of Medicine, Tokushima University, Tokushima, Japan; [c]Department of Anatomy II and Cell Biology, School of Medicine, Fujita Health University, Aichi, Japan; [d]Research Center for Stem Cell Engineering, National Institute of Advanced Industrial Science and Technology, Ibaraki, Japan; [e]Department of Plastic Surgery, School of Medicine, Jichi Medical University, Tochigi, Japan

Correspondence: Kotaro Yoshimura, M.D., Department of Plastic Surgery, University of Tokyo School of Medicine, 7-3-1, Hongo, Bunkyo-Ku, Tokyo 113-8655, Japan. Telephone: 81-3-5800-8948; E-Mail: kotaro-yoshimura@umin.ac.jp

Received March 2, 2015; accepted for publication August 10, 2015.

1066-5099/2015/$20.00/0

http://dx.doi.org/10.5966/sctm.2015-0037

ABSTRACT

Three-dimensional culture of mesenchymal stem/stromal cells for spheroid formation is known to enhance their therapeutic potential for regenerative medicine. Spheroids were prepared by culturing human adipose-derived stem/stromal cells (hASCs) in a non-cross-linked hyaluronic acid (HA) gel and compared with dissociated hASCs and hASC spheroids prepared using a nonadherent dish. Preliminary experiments indicated that a 4% HA gel was the most appropriate for forming hASC spheroids with a relatively consistent size (20–50 μm) within 48 hours. Prepared spheroids were positive for pluripotency markers (NANOG, OCT3/4, and SOX-2), and 40% of the cells were SSEA-3-positive, a marker of the multilineage differentiating stress enduring or Muse cell. In contrast with dissociated ASCs, increased secretion of cytokines such as hepatocyte growth factor was detected in ASC spheroids cultured under hypoxia. On microarray ASC spheroids showed upregulation of some pluripotency markers and downregulation of genes related to the mitotic cell cycle. After ischemia-reperfusion injury to the fat pad in SCID mice, local injection of hASC spheroids promoted tissue repair and reduced the final atrophy (1.6%) compared with that of dissociated hASCs (14.3%) or phosphate-buffered saline (20.3%). Part of the administered hASCs differentiated into vascular endothelial cells. ASC spheroids prepared in a HA gel contain undifferentiated cells with therapeutic potential to promote angiogenesis and tissue regeneration after damage. STEM CELLS TRANSLATIONAL MEDICINE *2015;4:1–12*

SIGNIFICANCE

This study shows the therapeutic value of human adipose-derived stem cell spheroids prepared in hyarulonic acid gel. The spheroids have various benefits as an injectable cellular product and show therapeutic potential to the stem cell-depleted conditions such as diabetic chronic skin ulcer.

INTRODUCTION

Human adipose-derived stem/stromal cells (hASCs) represent an abundant source of multipotent adult mesenchymal stem cells, which are easily obtained from subcutaneous adipose tissue via liposuction [1]. They can differentiate into not only adipocytes but also multiple lineages including osteogenic, chondrogenic [2], hepatogenic [3], myogenic [4], neurogenic [5], and angiogenic cell types [6, 7], although their differentiation potential appears to be generally limited. Recently, it has come to attention that human mesenchymal stem cells from the bone marrow, skin dermis, and adipose tissue contain a small fraction of privileged stem cells with greater plasticity, homing capacity, and higher stress resistance [8–10]. The selected cells, which are also called multilineage differentiating stress enduring (Muse) cells, are reported to divide symmetrically only when cultured under floating conditions and to form cell clusters. This result may also suggest that monolayer culture expansion gives rise only to cells with lower plasticity, although adherent monolayer culture is widely used to expand human bone marrow mesenchymal stem cells and

Published Ahead of Print on October 22, 2015 as 10.5966/sctm.2015-0037.

ASCs. Indeed, the expression of pluripotency makers or the differentiation potential of adult stem cells is known to gradually decrease over time during monolayer culture [11, 12].

Currently, the application of three-dimensional (3D) cell culture techniques for spheroid formation is receiving great interest, because stem cell spheroids tend to show higher therapeutic potential. Many studies have suggested that spheroid formation can boost functionality of stem cell components and avoid unfavorable migration when injected into local tissues. Several culture methods have been used to induce spheroid formation, including methods using a nonadherent specific dish [13–15], a spinner flask [16, 17], hanging drops [18, 19], and hydrogels [20, 21]. These methods facilitate cell-cell contacts and cell-matrix adhesion with the secreted extracellular matrix (ECM) [22]. By forming spheroids with native cell morphology, the cells show significant differences in pluripotent capacity compared with their counterparts cultured in a monolayer [23–25]. However, some issues for spheroid preparation remain to be optimized or resolved. If the size of spheroids is too large, central necrosis may develop, because the core of large spheroids will experience limited nutrient diffusion and severe hypoxia in vivo, particularly after injection into ischemic tissue [26, 27]. Additionally, inadvertent infusion of large spheroids into vessels can result in vascular thrombosis and aggravating an ischemic condition. Specific microplates for spheroid formation are commercially available, but the cost can be a concern depending on the number of spheroids to be prepared.

The aim of this study was to develop a simple and efficient method of spheroid preparation, which would provide a large amount of ASC spheroids with an appropriate and uniform size in a short time interval, for application in clinical ASC-based regenerative therapies. Because hyaluronic acid (HA) is a safe and histocompatible matrix [28] and is used for many clinical and research applications, such as an injectable carrier of stem cells and an injectable drug for cosmetic volumization or treating osteoarthritis, we used non-cross-linked HA gel for 3D culture preparation of hASC spheroids. In this study, we optimized the preparation method and investigated the biological properties and therapeutic potential of hASC spheroids prepared in a HA gel compared with monolayer-cultured hASCs.

Materials and Methods

Cell Isolation and Culture

Liposuction aspirates were obtained from healthy female donors (body mass index: 18–22) undergoing liposuction of the abdomen or thighs. Prior to the procedure, each patient provided her informed consent using an institutional review board-approved protocol. Human ASCs were isolated from the aspirated fat as described previously [29]. Briefly, the aspirated fat was washed with phosphate-buffered saline (PBS) and digested on a shaker at 37°C in PBS containing 0.075% collagenase for 30 minutes. Mature adipocytes and connective tissue were separated from cell pellets by centrifugation (760*g*, 5 minutes). The pellets were rinsed and resuspended after being filtered through 100-μm mesh. The suspension was disseminated at a density of 1.0×10^6 nucleated cells per 100-mm dish and cultured at 37°C in a humid 5% CO_2 atmosphere. The culture medium was Dulbecco's modified Eagle's medium (DMEM; Nissui, Tokyo, Japan, http://www.nissui-pharm.co.jp) supplemented with 10% fetal bovine serum (FBS). Primary cells were cultured for 7 days and were defined as passage 0. The medium was replaced three times per week. Cells were passaged every week with 0.25% trypsin, 2 mM EDTA for 5 minutes at 37°C. Cultured hASCs at passages 1 and 2 were used in the following experiments. Detailed characterization of the cultured hASCs used in this study was previously published [29].

3D Floating Culture in a HA Gel

HA gel was prepared by mixing HA powder and DMEM overnight on a plastic dish (Fig. 1A). The HA powder was a sterilized (pharmaceutical grade) product and non-cross-linked with an average molecular weight of 1,000 kDa (Kikkoman Biochemifa, Tokyo, Japan, http://biochemifa.kikkoman.co.jp). Suspended hASCs (in culture medium with the same volume as HA gel) were disseminated in the HA gel (1.0×10^4 cells per cm^2) and incubated (37°C, 5% CO_2) for 48 hours. Consequently, hASC spheroids were formed in the HA gel. For example, a 4% HA gel culture was prepared from 5% HA gel and a quarter volume of added cell suspension. To harvest the spheroids, medium was added to dilute HA gel, followed by incubation for 3 hours (37°C, 5% CO_2). The diluted supernatant containing hASC spheroids was collected in a silicon tube. ASC spheroids were obtained as a pellet from HA gel by three times dilution of HA gel with PBS and centrifugation (760*g*, 5 minutes).

As a preliminary experiment, various concentrations of HA gel (final concentrations: 0%, 2%, 3%, 4%, 5%, and 10%) were used. Suspended hASCs (1.0×10^4 cells per cm^2) were disseminated in each HA gel and observed for 7 days. Furthermore, for comparison, hASCs were also cultured on a nonadhesive dish (catalog no. 657970; Greiner Japan, Tokyo, Japan, http://www.greinerbioone.com) for spheroid formation.

Microarray Analysis

Samples were prepared as follows. Monolayer-cultured hASCs were harvested with 0.25% trypsin, 2 mM EDTA for 5 minutes at 37°C and were dissolved with Isogen (Wako, Osaka, Japan, http://www.wako-chem.co.jp) as a control sample. ASC spheroids were harvested after 48 hours of culture in 4% HA gel and were dissolved with Isogen as well. Total RNA was purified using the RNeasy mini kit (Qiagen Inc., Valencia, CA, http://www.qiagen.com) according to the manufacturer's recommendations. Fluorescently labeled cRNA was synthesized using a Quick Amp Labeling Kit (Agilent Technologies, Santa Clara, CA, http://www.agilent.com). Labeled cRNAs were hybridized with the SurePrint G3 human GE microarray 8 × 60K (G4851A; Agilent Technologies). Microarrays were scanned using a G2505C microarray scanner, and the results were analyzed using Feature extraction software (Agilent Technologies). Finally, we analyzed gene expression using GeneSpring GX 12.5 software (Agilent Technologies).

ELISA

Human ASC spheroids and monolayer-cultured hASCs were seeded at 1.0×10^5 cells in 60-mm dishes and cultured in DMEM with FBS for 24 hours (37°C, 5% CO_2). Subsequently, the medium was exchanged for DMEM without FBS, and each dish was incubated under hypoxic (1% O_2) or normoxic (6% O_2) conditions. After 48 hours, the culture media were collected and filtered (0.22-μm filter, Millex-GV filter; Millipore, Billerica, MA, http://www.millipore.com). Enzyme-linked immunosorbent

Published Ahead of Print on October 22, 2015 as 10.5966/sctm.2015-0037.

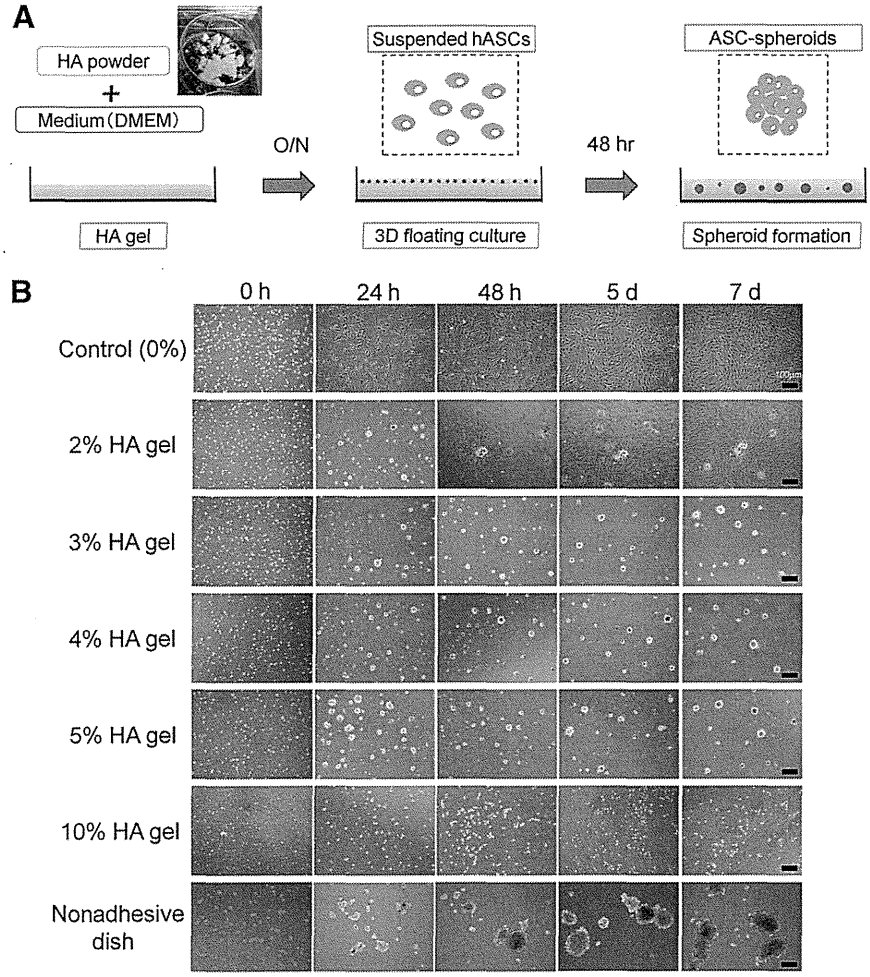

Figure 1. Three-dimensional floating culture in HA gel. **(A):** First step (left). HA gel is prepared by mixing sterilized HA powder and culture medium (DMEM) overnight. Middle: Second step. Human ASCs (1.0×10^4 cells per cm^2) are disseminated on the HA gel. Right: Final step. After incubation for 48 hours (37°C, 5% CO_2), ASCs formed spheroids in the gel. For retrieval, culture medium is added to dilute HA gel and incubated for 3 hours. The diluted supernatant containing ASC spheroids is transferred into a silicon tube, and ASC spheroids are collected as a pellet by centrifugation (760*g*, 5 minutes). **(B):** Three-dimensional culture in HA gels (0%, 2%, 3%, 4%, 5%, or 10%) or on a nonadhesive dish. Human ASCs were seeded in the HA gels of various (0%–10%) concentrations. In 2%–3% HA gel ASC formed spheroids, but some of them sank and proliferated on the bottom of the dish like an explant culture. In contrast, in 4%–5% HA gel formation of floating spheroids was completed at 48 hours without further substantial change in size afterward. Spheroids were not formed in 10% HA gel. On a nonadhesive dish ASC spheroids continued growing until day 7. Scale bars = 100 μm. Abbreviations: 3D, three-dimensional; ASC, adipose-derived stem/stromal cell; d, day(s); DMEM, Dulbecco's modified Eagle's medium; h or hr, hour(s); HA, hyaluronic acid; hASCs, human adipose-derived stem/stromal cells; O/N, overnight.

assay (ELISA) kits (Ray Biotech, Inc., Norcross, GA, http://www.raybiotech.com) for hepatocyte growth factor (HGF), vascular endothelial growth factor (VEGF), epidermal growth factor (EGF), platelet-derived growth factor (PDGF-BB), and basic fibroblast growth factor (bFGF) were used. The absorbance was spectrophotometrically measured at 450 nm using an infinite microplate reader (M1000; Tecan Group, Männedorf, Switzerland, http://www.tecan.com).

Immunostaining of Spheroids for Stem Cell Markers

Prepared hASC spheroids were embedded in OCT compound (Sakura Finetek, Tokyo, Japan, http://www.sakura-finetek.com). Cryopreserved samples were cut at 8-μm thickness and immunostained after fixation with 4% paraformaldehyde. The following primary antibodies were used for immunohistochemistry: rabbit anti-NANOG antibody (GeneTex, Irvine, CA, http://www.genetex.com), rabbit anti-OCT3/4 antibody (GeneTex), rabbit anti-SOX2 antibody (GeneTex), rat anti-SSEA-3 antibody (Millipore), and mouse anti-CD90 antibody (Biolegend, San Diego, CA, http://www.biolegend.com). These primary antibodies were detected with Alexa Fluor 568-conjugated anti-rabbit IgG (Molecular Probes, Carlsbad, CA, http://probes.invitrogen.com), fluorescein isothiocyanate-conjugated anti-rat IgM (Jackson ImmunoResearch, West Grove, PA, http://www.jacksonimmuno.com), and Alexa Fluor 488-conjugated anti-mouse IgG (Molecular Probes). Samples were incubated with blocking solution containing 5% FBS and 0.1% Triton X-100 (Sigma-Aldrich, St. Louis, MO, http://www.sigmaaldrich.com) in PBS at room temperature for 60 minutes. Samples were then incubated with primary antibodies overnight at 4°C. After three washes with PBS, samples were incubated with secondary antibodies for 60 minutes at room temperature. Nuclei were stained with Hoechst 33342 (Dojindo, Kumamoto, Japan, http://www.dojindo.com). All images were taken with

Published Ahead of Print on October 22, 2015 as 10.5966/sctm.2015-0037.

fluorescent microscopy (Keyence, Osaka, Japan, http://www.keyence.com) using the same laser intensity and detection sensitivity.

Mouse Model for Ischemia-Reperfusion Injury to Adipose Tissue

Ten- to twelve-week-old male severe combined immunodeficient (SCID) mice (C.B-17/Icr-scid/scidJcl) were purchased from CLEA Japan, Inc. (Tokyo, Japan, http://www.clea-japan.com). All animal experiments were performed with approval from the Institutional Animal Care and Use Committee of the University of Tokyo. After SCID mice were fasted for 24 hours, they were anesthetized with inhaled isoflurane, and a 1.5-cm skin incision was made in the inguinal region. Under a surgical microscope, the subcutaneous inguinal fat pad was elevated with the main nutrient vessels arising from the femoral vessels intact. The nutrient vessels were clamped with a vessel microclip for 4 hours to induce temporary ischemia. This injury and repair model is reliable to see the wound-healing process as previously published [30]. Immediately after the vessels were released to allow reperfusion, 200 μl of treatment solution was injected with a 30-gauge needle into the fat pad at three points. The treatment solution was PBS (n = 6), monolayer-cultured hASCs (n = 6), or hASC spheroids (n = 6). The dissociated hASCs were obtained by conventional monolayer culture (5.0×10^5 cells per 10-cm dish) for 48 hours. By contrast, hASC spheroids were obtained by 3D floating culture (5.0×10^5 cells per 10-cm dish) in a 4% HA gel for 48 hours. The cultured hASCs obtained from a single subject were used in the animal experiment. The adipose tissue samples were harvested carefully under the surgical microscope at various intervals (at 7, 14, and 28 days) after ischemia-reperfusion injury, weighed, and examined by immunohistochemistry. Therapeutic effects were evaluated with a "tissue repair score," which was calculated by multiplying the survival area ratio and the relative weight of the fat pad. The survival area ratio is the percentage of perilipin-positive area in the histological cross-sections of the tissue, and the relative weight of the fat pad is (weight of fat pad)/(weight of body).

Immunostaining of Adipose Tissue

Harvested adipose tissue samples were zinc-fixed (Zinc Fixative; BD Biosciences, San Jose, CA, http://www.bdbiosciences.com) and paraffin-embedded. The samples were sectioned at 5 μm and subjected to the following staining procedures. The following primary antibodies were used for immunohistochemistry: guinea pig anti-perilipin antibody (Progen Biotechnik, Heidelberg, Germany, http://www.progen.de), rat anti-MAC-2 antibody (Cedar Lane Laboratories, Burlington, Canada, http://www.cedarlanelabs.com), anti-58K human Golgi protein antibody (Abcam, Cambridge, U.K., http://www.abcam.com). Isotypic antibodies were used as a negative control for each immunostaining. Alexa Fluor 488- or 568-conjugated secondary antibodies (Molecular Probes) were used for visualization. Vessels (vascular endothelial cells) were stained with Alexa Fluor 594-conjugated isolectin GS-IB_4 (Molecular Probes), and nuclei were stained with Hoechst 33342 (Dojindo). All images were captured with fluorescent microscopy (Keyence, Osaka, Japan) using the same laser intensity and detection sensitivity. The area composed of perilipin-negative (dead adipocytes) or perilipin-positive (viable adipocytes) cells was evaluated by image analysis software (Photoshop CS6; Adobe Systems, San Jose, CA, http://www.adobe.com).

Statistical Analysis

The results were expressed as the means ± SD. Comparisons between the two groups were performed with Welch's t test. Comparisons of multiple groups were done by Tukey's tests. A value of $p < .05$ was considered statistically significant.

RESULTS

Appropriate Concentration of HA Gel for 3D Floating Culture

Suspended hASCs were disseminated in each well of a 6-well dish (1.0×10^4 cells per cm^2) filled with various concentrations of HA gel (Fig. 1B). In 2%–3% HA gels, some ASCs and ASC spheroids sunk to the bottom of the dish and then proliferated on the dish. In contrast, in 4%–5% HA gel hASCs did not sink; spheroid formation was completed within 48 hours, and the spheroid size did not change substantially afterward. No spheroid was formed in the 10% HA gel. Based on the above results, 3D culture in 4% HA gel for 48 hours was used for hASC spheroid preparation in the following experiments. On the nonadhesive dish, hASCs formed spheroids but continued growing until 7 days resulting in spheroids of very variable size.

Morphological Difference in Spheroids Prepared by HA Gel and on a Nonadhesive Dish

Human ASC spheroids were prepared using either 3D culture in a HA gel or nonadhesive dish culture for 48 hours (Fig. 2A). The histograms of spheroid diameter showed that hASC spheroids formed in a HA gel presented a unimodal distribution with relatively small (approximately 30 μm) size (Fig. 2B). On the other hand, hASC spheroids formed on a nonadhesive dish showed a bimodal distribution (with peaks at 20–60 and 100–200 μm). Cell proliferation was relatively suppressed in spheroid formation by 3D culture in the HA gel or on a nonadhesive dish compared with monolayer culture (Fig. 2C).

Microarray (Monolayer Culture vs. 3D Floating Culture in HA Gel)

Microarray analyses were performed to analyze differences in gene expression between monolayer-cultured hASCs and hASC-spheroids prepared by 3D culture in the HA gel. Spheroid formation promoted gene expression of some angiogenesis-related growth factors (*VEGFA, VEGFB, HGF, PDGFA, PDGFC*), anti-inflammatory factors (*IL1RN, IL11,* etc.) and pluripotent stem cell markers (*NANOG, OCT3/4, STAT3,* etc.) compared to monolayer culture (Fig. 3). In addition, gene expression related to the mitotic cell cycle was generally decreased by spheroid formation in the HA gel.

ELISA for Angiogenic Growth Factors

ELISA results indicated that secretion of VEGF, HGF, and EGF, but not PDGF-BB, generally increased under hypoxic conditions in nonspheroid and spheroid hASCs (supplemental online Fig. 1). Spheroid hASCs showed greater secretion of HGF than nonspheroid hASCs under both normoxic and hypoxic conditions. PDGF-BB secretion did not differ between the groups. In addition,

Published Ahead of Print on October 22, 2015 as 10.5966/sctm.2015-0037.

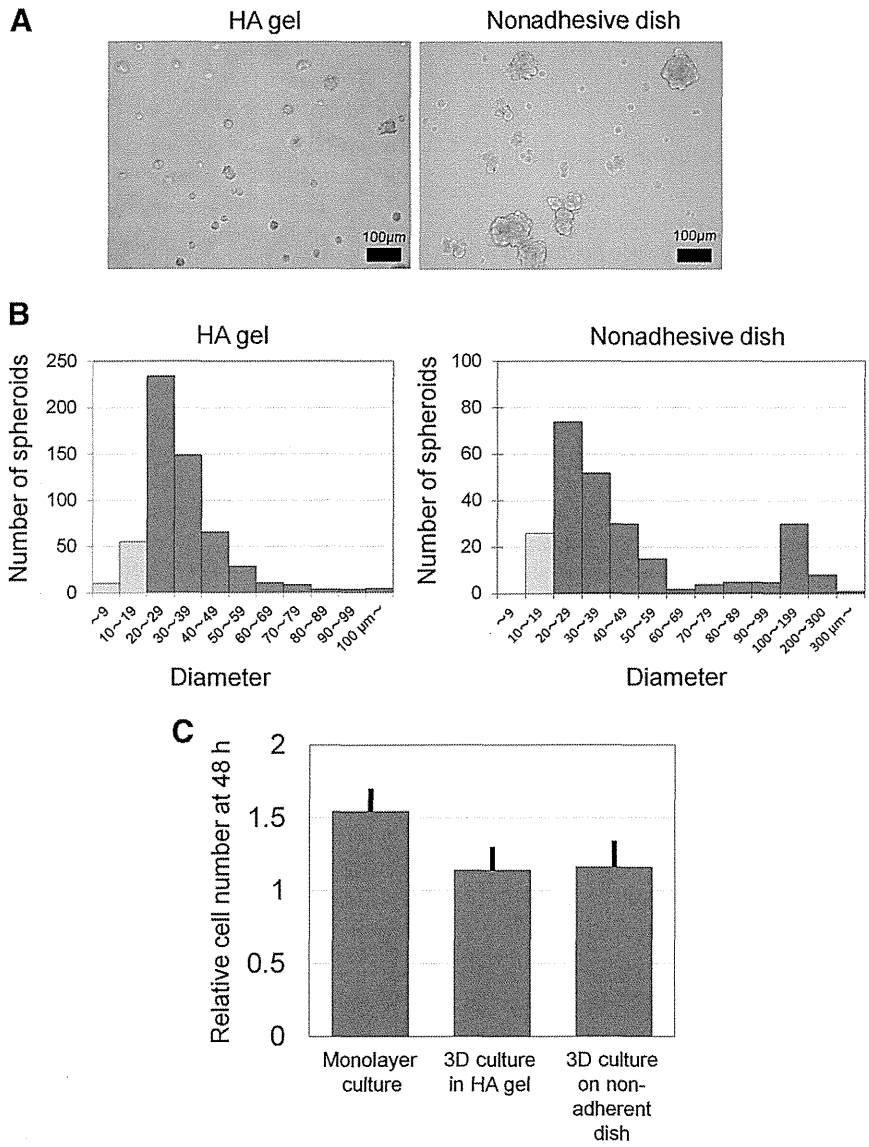

Figure 2. Differences between spheroids prepared in a HA gel and on a nonadherent dish. **(A):** Microscopic images of adipose-derived stem/stromal cell (ASC) spheroids that were prepared by 48-hour 3D culture in 4% HA gel or on a nonadherent dish. Scale bars = 100 μm. **(B):** Representative histograms of ASC spheroid diameter prepared in 4% HA gel or on a nonadherent dish. Cell aggregates with a diameter >20 μm were regarded as spheroids (blue). In the HA gel the spheroid diameter showed a unimodal distribution and was relatively small. By contrast, the diameter showed bimodal distribution on the nonadhesive dish, and a substantial number of ASC spheroids were >100 μm in diameter. Abbreviations: 3D, three-dimensional; h, hour(s); HA, hyaluronic acid.

bFGF secretion was at an undetectable level in all groups (data not shown).

Stem Cell Marker Expression of hASC Spheroids

Spheroids of hASCs prepared in the HA gel were orbicular, and their surface looked smooth (Fig. 4A). Immunocyto-/histochemistry indicated that all hASCs expressed CD90 in monolayer culture, nonadherent spheroid culture, and HA-gel spheroid culture (Fig. 4B). It was also indicated that ASC spheroids expressed various stem cell markers such as NANOG, OCT3/4, and SOX-2 (Fig. 4C). SSEA-3, which is a specific marker of Muse cells, was expressed only ~1% of hASCs in monolayer culture, but it was more highly expressed spheroid culture, especially in hASC spheroids prepared in HA gel (Fig. 4D). Approximately 40% of the spheroids were rich in SSEA-3-positive hASCs (Fig. 4E).

Wound Healing Process After Ischemia-Reperfusion Injury of Inguinal Fat Pad and Therapeutic Effects of Monolayer-Cultured or Spheroid ASCs

The inguinal fat pads of SCID mice underwent ischemia-reperfusion injury (Fig. 5A) and were harvested 7, 14, or 28 days after the injury. After the injury, numerous adipocytes were killed and became oil droplets (perilipin-negative round areas) of various sizes (depending on the number of dead adipocytes) that were later surrounded by infiltrated MAC-2-positive macrophages for phagocytosis (crown-like structure) by day 7 (degeneration phase; Fig. 5B). Thereafter, the injury activated

Published Ahead of Print on October 22, 2015 as 10.5966/sctm.2015-0037.

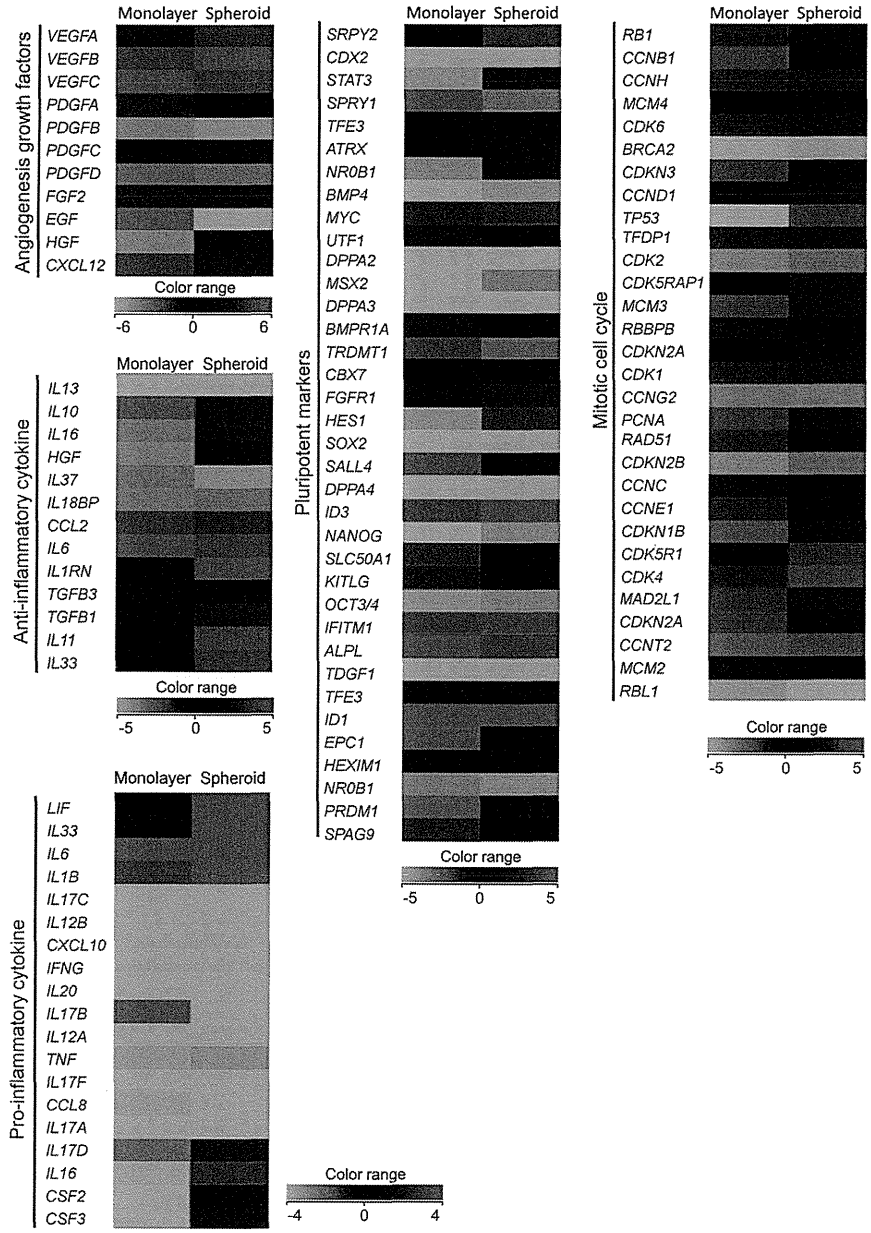

Figure 3. Microarray analysis of human adipose-derived stem/stromal cells (ASCs) prepared by monolayer culture versus ASC spheroids by three-dimensional culture in hyaluronic acid gel. ASC spheroids showed increased gene expression of some angiogenic growth factors (*VEGFA, VEGFB, HGF, PDGFA, PDGFC*), anti-inflammatory factors *(IL1RN, IL11*, etc.), and pluripotent markers (*NANOG, OCT3/4, STAT3*, etc.) compared with monolayer-cultured ASCs. In contrast, gene expression related to the mitotic cell cycle decreased thoroughly in ASC spheroids.

tissue-resident stem/progenitor cells such as mouse ASCs, which then started to differentiate into adipocytes (perilipin-positive small adipocytes) by day 14. The regeneration process including adipogenesis and angiogenesis was clearly seen on day 14 in all samples (regeneration phase). Tissue degeneration looked similar among all treated groups on day 7, but tissue regeneration happened more quickly and consistently in hASC-treated or hASC spheroid-treated samples compared with PBS-treated controls on day 14. Indeed, immunohistology after 28 days indicated that the tissue was well-filled with intact size adipocytes, and wound healing looked complete in samples treated with hASCs or hASC spheroids, although PBS-treated samples still showed the typical features of ongoing wound healing such as lipid droplets and small immature adipocytes. Viable adipocyte area (perilipin-positive area), as well as the total area, was measured, and the calculated qualitative data indicated a significant difference in the tissue viability and wound healing process among the groups (Fig. 5C).

Quantitative evaluation of wound healing from the injury was also performed. The gross weight of the fat pad and the whole body was measured (Fig. 6A). PBS-treated samples gradually atrophied over time and were smallest among the treatment groups on day 7, 14, and 28. The relative weight of hASC spheroid-treated samples recovered quickly after day 14 and was significantly larger compared with the other groups on day 28. Overall tissue repair was scored by multiplying the survival area ratio and the

Published Ahead of Print on October 22, 2015 as 10.5966/sctm.2015-0037.

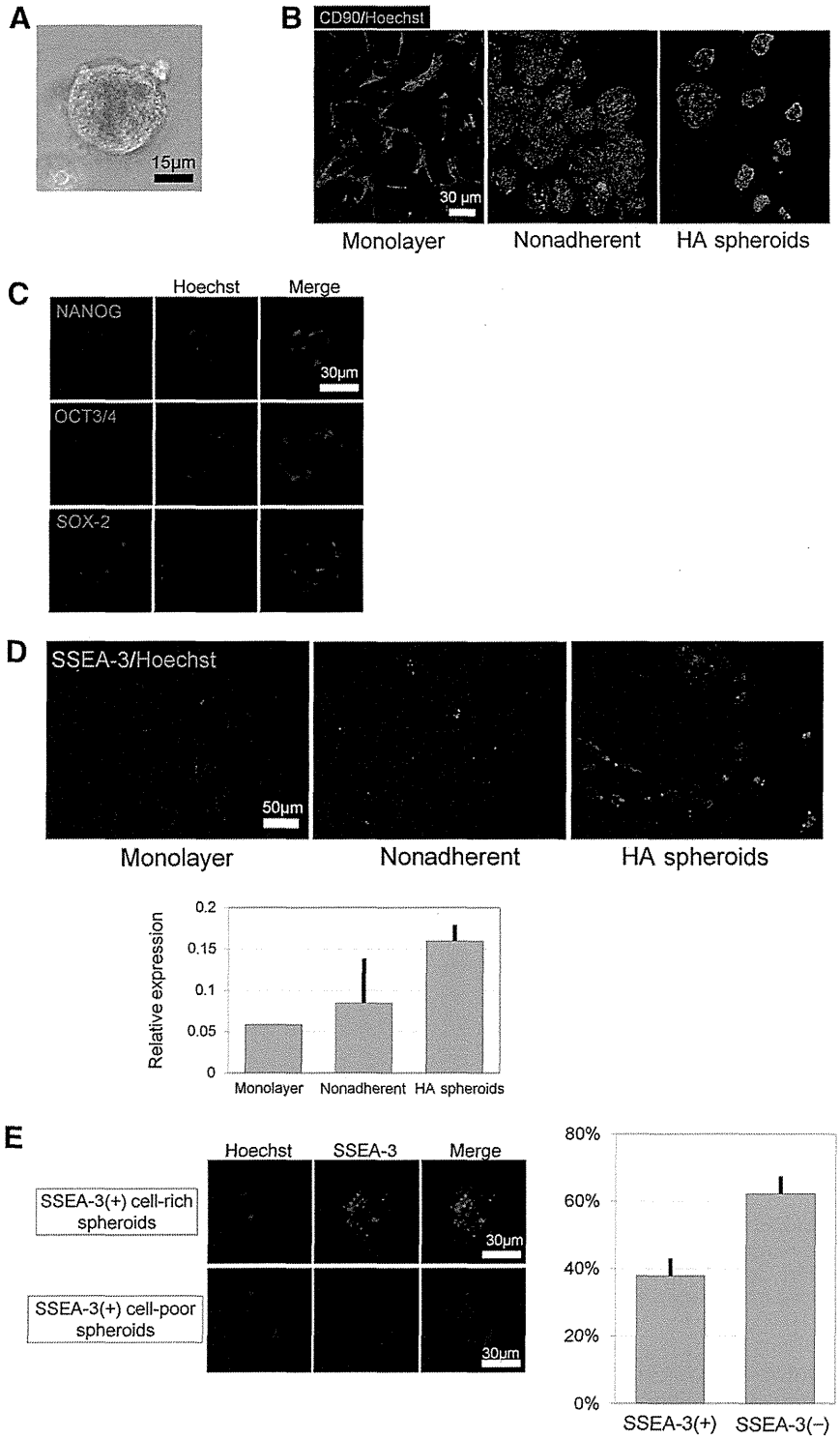

Figure 4. Immunostaining of adipose-derived stem/stromal cell (ASC) spheroids prepared in HA gel. **(A):** Microscopically, spheroids were consistently orbicular in shape and had a smooth surface. Scale bar = 15 μm. **(B):** Immunocyto-/histochemistry for CD90. CD90 was expressed by almost all cells in monolayer, nonadherent, and HA spheroids. Scale bar = 30 μm. **(C):** Representative immunostaining of cryosections. ASC spheroids expressed pluripotent stem cell markers such as NANOG, OCT3/4, and SOX-2. Scale bar = 30 μm. **(D):** Immunocyto-/histochemistry for SSEA-3. SSEA-3 was most highly expressed by HA spheroids compared with monolayer-cultured ASCs and nonadherent culture spheroids. Scale bar = 50 μm. **(E):** Some of the ASC spheroids were positive for SSEA-3, a pluripotent stem cell (muse cell) marker. SSEA-3(+)-rich spheroids constituted approximately 40% of ASC spheroids. Scale bars = 30 μm. Abbreviation: HA, hyaluronic acid.